Vol. 49

Bollettino di Geofisica teorica ed applicata

An International Journal of Earth Sciences

N. 2 SUPPLEMENT

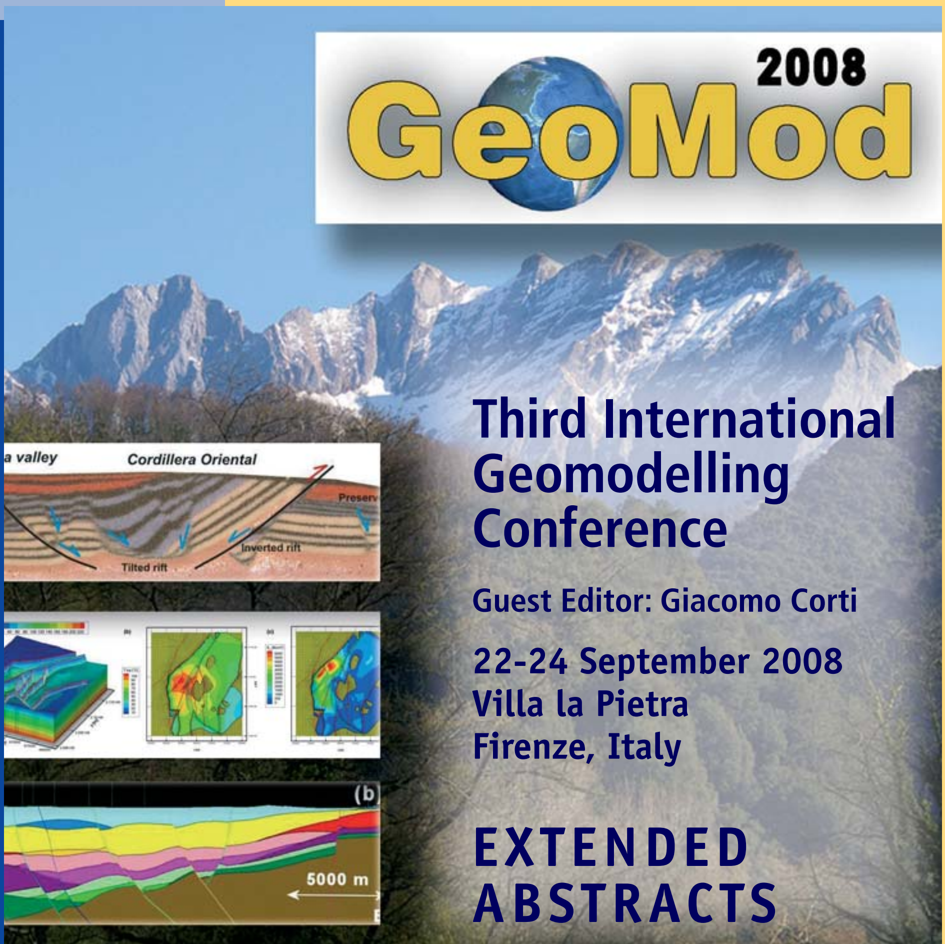

Third International Geomodelling Conference

Guest Editor: Giacomo Corti

22-24 September 2008
Villa la Pietra
Firenze, Italy

EXTENDED ABSTRACTS

Istituto Nazionale di Oceanografia
e di Geofisica Sperimentale

112, 1091-1105.

Iaffaldano G., Bunge H.-P. and Dixon T.H.; 2006: *Feedback between mountain belt growth and plate convergence*. Geology, 34, 893-896.

Iaffaldano G. and Bunge H.-P.; 2008: *Strong plate coupling along the Nazca/South America convergent margin*. Geology, 36, 443-446.

Isacks B.L.; 1988: *Uplift of the central Andean plateau and bending of the Bolivian orocline*. Journal of Geophysical Research, 93, 3211–3231.

Kong X. and Bird P.; 1995: *SHELLS: A thin-shell program for modeling neotectonics of regional or global lithosphere with faults*. Journal of Geophysical Research, 100, 22129–22132.

Llenos A.L. and McGuire J.J.; 2007: *Influence of fore-arc structure on the extent of great subduction zone earthquakes*. Journal of Geophysical Research, 112, B09301.

Müller R.D., Sdrolias M., Gaina C. and Roest W.R.; 2008: *Age, spreading and spreading asymmetry of the world's ocean crust*. Geochemistry Geophysics Geosystems, 9, Q04006.

National Geophysical Data Center; 1998: Digital relief of the surface of the Earth. Boulder, Colorado, National Oceanic and Atmospheric Administration Data Announcement 88-MGG-02.

Norabuena E.O., Dixon T.H., Stein S. and Harrison C.G.A.; 1999: *Decelerating Nazca-South America and Nazca-Pacific plate motions*. Geophys.ical Research Letters, 26, 3405-3408.

Russo R.M. and Silver P.G.; 1994: *Trench-parallel flow beneath the Nazca plate from seismic anisotropy*. Science, 263, 1105–1111.

Sandwell D.T. and Smith W.H.F.; 1997: *Marine gravity anomalies from Geosat and ERS 1 satellite altimetry*. Journal of Geophysical Research, 102, 10039-10054.

Schellart W.P., Freeman J., Stegman D.R., Moresi L. and May D.; 2007: *Evolution and diversity of subduction zones controlled by slab width*. Nature, 446, 308–311.

Sella G.F., Dixon T.H. and Mao A.; 2002: *REVEL: A model for recent plate velocities from space geodesy*. Journal of Geophysical Research, 107.

Smith W.H.F. and Sandwell D.T.; 1997: *Global sea floor topography from satellite altimetry and ship depth soundings*. Science, 277, 1956-1962.

Song T.R.A. and Simons M.; 2003: *Large trench-parallel gravity variations predict seismogenic behavior in subduction zones*. Science, 301, 630-633.

Tackley P.J., Stevenson D.J., Glatzmaier G.A. and Schubert G.; 1994: *Effects of multiple phase transitions in a three-dimensional spherical model of convection in Earth's mantle*. Journal of Geophysical Research, 99, 15877–15902.

Zhong S., Zuber M.T., Moresi L. and Gurnis M.; 2000: *Role of temperaturedependent viscosity and surface plates in spherical shell models of mantle convection.* Journal of Geophysical Research, 105, 11063–11082.

A NUMERICAL STUDY ON THE EFFECTS OF SURFACE BOUNDARY CONDITION AND RHEOLOGY ON SLAB DYNAMICS

B.J.P. Kaus[1,2], T.W. Becker[2]

[1] *Geophysical Fluid Dynamics, ETH Zurich – Schaffmattstrasse 30, 8093 Zurich (Switzerland)*
[2] *Department of Earth Sciences, University of Southern California, Los Angeles (USA)*

Summary

Numerical models of free-slab subduction that employ viscous rheologies and a free-slip surface boundary condition result in slabs that 'drip-off' rather than subduct. Since this appears unrealistic, a depth-dependent Byerlee-type viscoplastic slab rheology is typically used instead. Here, we study the effects of rheology (viscous versus viscoplastic) and surface boundary condition (free-surface versus free-slip) on subduction dynamics. Results confirm confirm the ad hoc assumptions and conclusions from a previous visco-plastic study with free-slip. They also show that the presence of free-surface causes viscous slabs to subduct like observed in laboratory experiments, and that models with a free-slip/Byerlee rheology behave similar to models with a free surface and viscous rheology. Finally, we study the effects of varying slab/mantle viscosity contrasts and slab thickness on subduction dynamics, and show that the

rich behaviour known from laboratory experiments arises naturally in numerical models that have a free-surface.

Introduction

A number of studies have addressed the dynamics of subduction with 2D and 3D numerical models [*Schmeling et al.*, submitted] or with laboratory experiments. Whereas laboratory experiments exhibit slab-like behaviour for purely viscous rheologies, numerical experiments typically employ (slab) viscosities of the type

$$\frac{1}{\eta_{eff}} = \frac{1}{\eta_n} + \frac{1}{\eta_{yield}} \text{ (i), or } \eta_{eff} = \min(\eta_n, \eta_{yield}) \text{ (ii)}$$

where η_{eff} is the effective viscosity, η_n the Newtonian viscosity and η_{yield} the plastic viscosity, given by

$$\eta_{yield} = \frac{(\tan(\phi)\rho g z + c)\lambda}{2\dot{\varepsilon}_{II}}$$

where $\dot{\varepsilon}_{II}$ denotes the second invariant of the strain rate tensor, ρ slab-density, g gravitational acceleration, z depth below the surface, c cohesion, ϕ friction angle and λ the pore fluid pressure. Results show that 'realistic' slab behaviour occurs if λ~0.1 (corresponding to effective angles of friction of ~3^o). If λ=0.01(0.3^o), slab break-off occurs soon after model start, and if λ=1(30^o) the slab fails to detach from the upper, free-slip, boundary and drips-off in a Rayleigh-Taylor like mode [*Enns et al.*, 2005]. Whereas the use of a Byerlee-type rheology is certainly justified if compared to nature, it remains an open question whether the values employed in the numerical models can be compared to natural values (which would in that case indicate that extremely small angles of internal friction are required for subduction to occur). It is also interesting that laboratory models of subduction do not require Byerlee-type rheologies for 'realistic' slab behaviour. To obtain an insight in the differences between the two methods, we here summarize the results of a numerical study in which we addressed the effects of rheology and surface boundary condition on subduction dynamics.

Numerical model

We solve the conservation equations of mass and momentum for slowly moving, incompressible, visco-elasto-plastic rheologies with a 2D finite element code called MILAMIN_VEP. MILAMIN_VEP is based on the viscous flow solver MILAMIN [*Dabrowski et al.*, 2008] that was extended to allow for visco-elasto-plastic rheologies, tracer-based advection, phase transitions, remeshing and thermo-mechanical coupling. Since MILAMIN employs unstructured triangular finite elements, it is possible to use a dense mesh in the vicinity of the trench region, and a much coarser mesh elsewhere, which greatly reduces the computational cost. Here, we mainly focus on the setup that was studied by Enns et al. [2005], in which a slab was emplaced in a viscous mantle, and the effects of the overriding plate are ignored. Since in this case the mantle is allowed to flow on top of the slab, special care is required for the numerical treatment of the trench area (in particular, since elements may 'overturn' in the trench region). We therefore employ a mass-conservative algorithm that remeshes the free surface if the trench angle exceeds a critical angle (typically $10\text{-}20^o$ – results are relatively insensitive to the exact value employed). Benchmarks of this code with a number of other codes, and with laboratory experiments for subduction, are presented in Schmeling et al. [submitted].

Results

Comparison with previous, visco-plastic, results.

Enns *et al.* [2005] studied the dynamics of subducting slabs in a 2D setup with free-slip upper boundary conditions, and demonstrated that the Byerlee rheology yields a slab-like behaviour if λ is tuned accordingly. We have repeated some of their experiments with MILAMIN_VEP and with a slightly different initial setup (using a straight rather than curved initial slab) and a different implementation of plasticity (method ii instead of method i). The results are very similar (Fig. 1), which gives confidence in the numerical code employed here. Moreover, it demonstrates that details of plasticity implementation

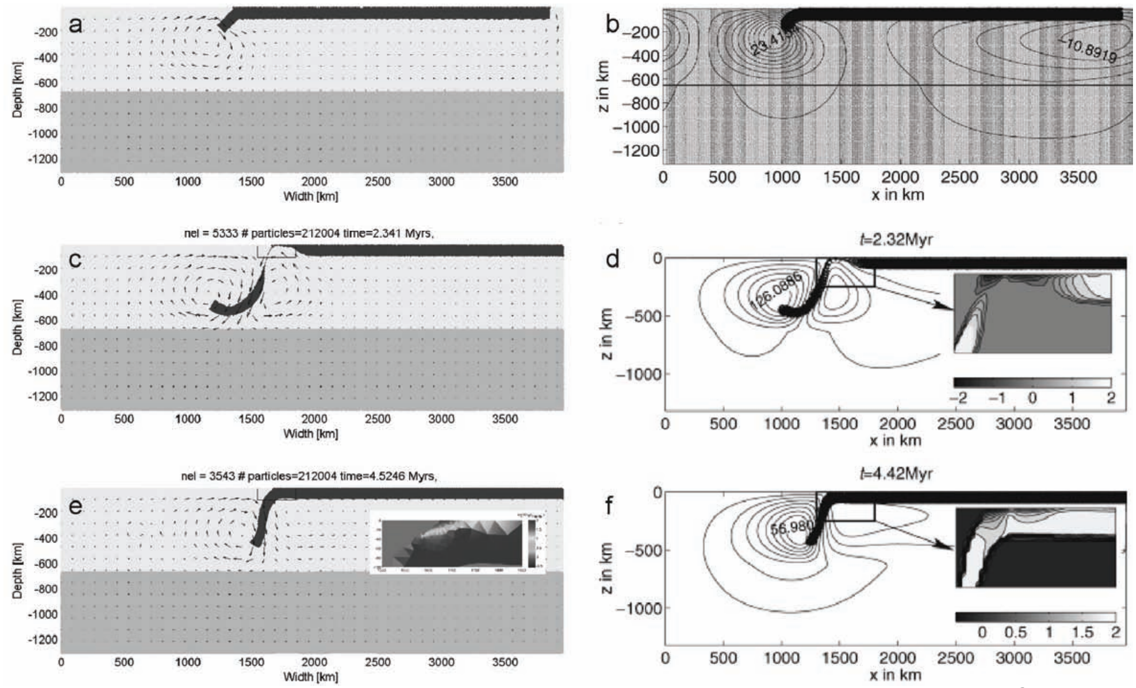

Figure 1. Comparison with the results of Enns *et al.* [2005]. Parameters employed are ρ_{slab}=3300 kg/m^3, μ_{slab}=10^{22} Pas, ρ_{mantle}=3250 kg/m^3, μ_{mantle}=10^{20} Pas, μ_{low_mantle}=5.10^{21} Pas. The slab has a thickness of 99 km, a viscoplastic rheology (c=60MPa, ϕ=30^o) and is attached to the right boundary. The mantle is linear viscous, and boundary conditions are free slip on all sides. a) & b) initial setup for MILAMIN_VEP respectively FDCON simulations (for free slab runs; c-f describe cases in which the slab is attached to the right side of the box). c) & d) results for simulations with λ=0.01. e) & f) results with λ=0.1. Right column are results from Enns *et al.* [2005].

(method i of ii) do not drastically alter results [see also *Becker and Faccenna*, in press]. Slab-like behaviour is obtained if λ=0.1. Note that in this case plasticity reduces slab viscosity only at the location where the slab 'detaches' from the upper, free-slip, boundary.

Free surface versus free slip.

Whereas one can argue that viscoplastic rheologies might be a more realistic approximation of the lithosphere, it remains unclear how viscoplastic simulations compare to laboratory experiments and whether the employed parameters (in particular λ) can be interpreted as physical parameter. For this reason we have performed a set of runs in which viscoplastic/free slip setups are compared with viscous/free surface setups (similar to laboratory experiments). Results (Fig. 2) show that the geometries are in both cases very similar. This suggests that the main effect of a Byerlee-type rheology is to mimic a free-surface. It is also suggests that previous modelling results with Byerlee-type rheologies in combination with free-slip upper boundary conditions did a reasonable job in representing the dynamics of subduction. Thus, plasticity in those previous models should be regarded as a numerical trick that helps detachment of the slab from the free surface, as was argued by Enns *et al.* [2005]. Specifically, when tuned correctly, the plasticity trick will not strongly affect the partitioning of viscous dissipation between slab and mantle which has received a lot of attention in studies of subduction velocities. It should however also be noted that creating topography at the trench consumes energy. This factor, which scales with the density contrast between rocks and air/water, is absent in free-slip subduction simulations.

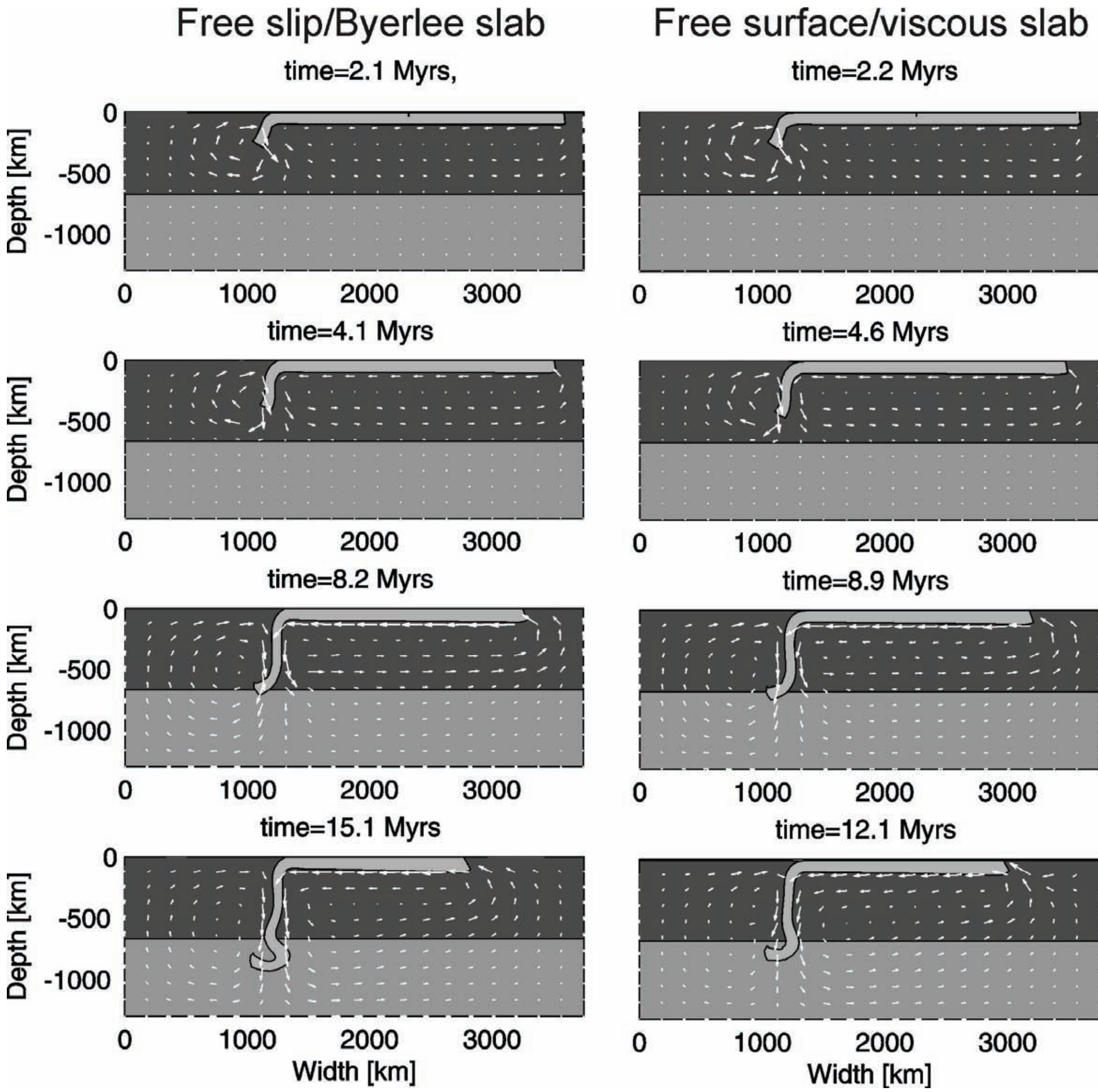

Figure 2. Comparison of results with a free slip upper boundary condition and a Byerlee-type slab rheology with λ=0.1 (left), and with results that have a viscous slab and a free surface upper boundary condition (right). Parameters for the free-slip model are as in Fig. 1e.

Effects of slab thickness and viscosity contrast on the dynamics of subduction

The results of a number of free-surface simulations, in which the slab thickness and viscosity have been varied, are presented in figure 3. If the viscosity contrast between slab and mantle is smaller than ~10, slabs ‘drip-off’ and do not behave in a plate-like coherent manner (i.e. the surface velocity along the slab is not constant, but increases strongly in the vicinity of the trench) . If viscosity contrasts are sufficiently large, slabs behave in a plate-like manner and have a nearly constant surface velocity. Plate-like slabs induce large-scale motion in the upper mantle, whereas drip-like slabs induce flow on smaller length scales. Slabs with a viscosity contrast of ~100 descend nearly vertical through the upper mantle and fold upon penetration of the 660 km transition (with a wavelength that decreases with decreasing slab thickness as expected from folding theory). Stiff slabs (viscosity contrast > 1000) bend in the upper mantle and result in forward trench motion once the slab tip arrives at the 660 km transition.

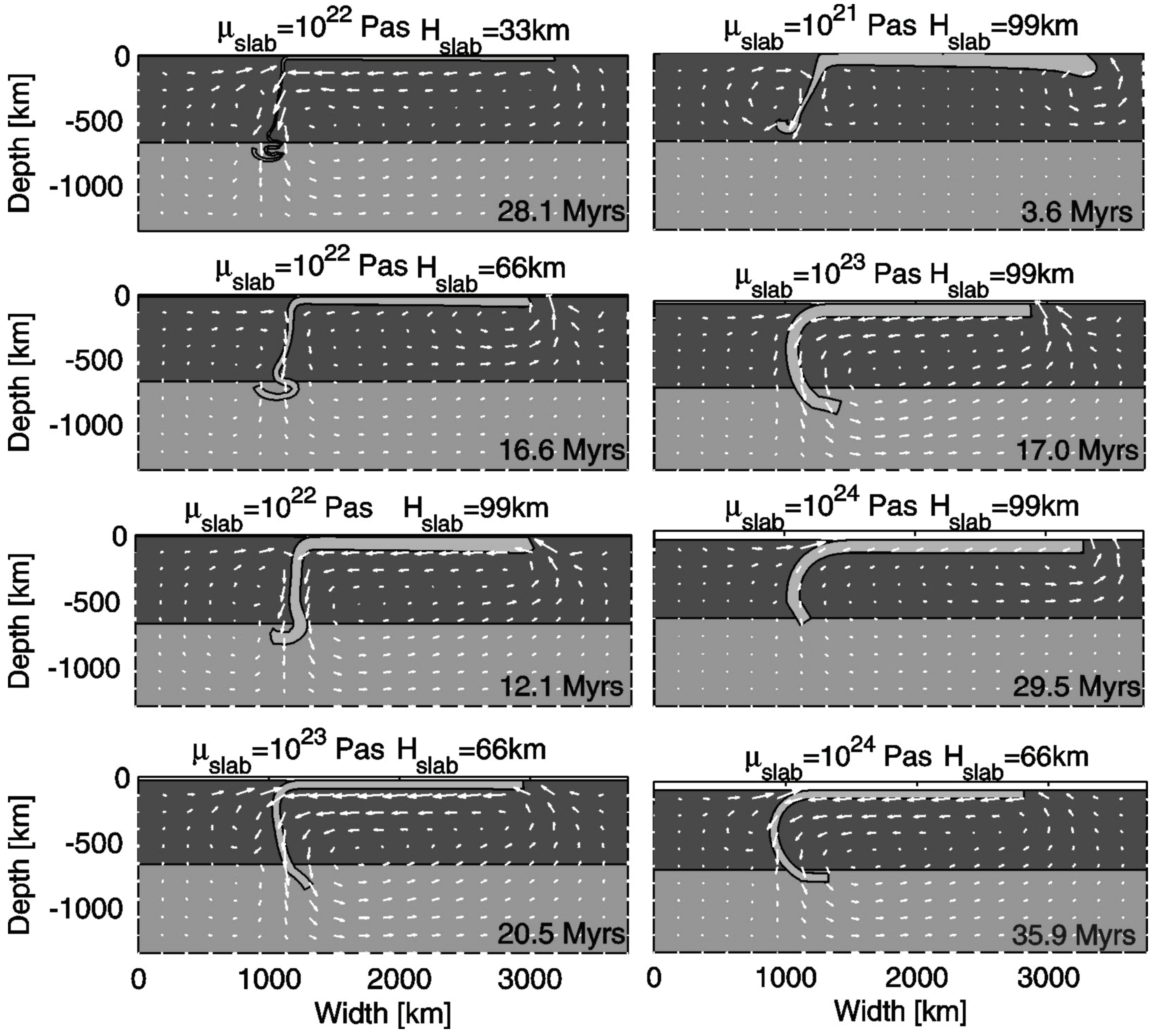

Figure 3. Effect of slab thickness and viscosity on the dynamics of subduction. All runs are performed with a free surface and a linear viscous rheology. Other parameters as in Fig. 1.

These numerical simulations are in general agreement with the results from laboratory experiments [e.g. *Bellahsen et al.*, 2005; *Funiciello et al.*, in press; *Schellart*, 2008; *Schmeling et al.*, submitted], which highlighted that importance of slab/mantle viscosity ratios for relative trench motions.

REFERENCES

Becker, T. W., and C. Faccenna (in press), A review of the role of subduction dynamics for regional and global plate motions., *International Journal of Earth Sciences. , Special Volume: Subduction Zone Geodynamics.*

Bellahsen, N., et al. (2005), Dynamics of subduction and plate motion in laboratory experiments: Insights into the "plate tectonics" behavior of the Earth, *J. Geophys. Res.-Solid Earth*, *110*(B1), -.

Dabrowski, M., et al. (2008), MILAMIN: MATLAB-based FEM solver for large problems., *Geochem. Geophys. Geosyst.*, doi:10.1029/2007GC001719.

Enns, A., et al. (2005), The dynamics of subduction and trench migration for viscosity stratification, *Geophysical Journal International*, *160*(2), 761-775.

Funiciello, F., et al. (in press), Trench migration, net rotation and slab - mantle coupling, *Earth Planet.Sci.Lett.*

Schellart, W. P. (2008), Kinematics and flow patterns in deep mantle and upper mantle subduction models: Influence of the mantle depth and slab to mantle viscosity ratio, *Geochem. Geophys. Geosyst.*, *9*, -.

Schmeling, H., et al. (submitted), A benchmark comparison of spontaneous subduction models: towards a free surface., *Phys.Earth Planet.Inter.*

FROM LONGITUDINAL SLAB CURVATURE TO SLAB RHEOLOGY

C. Loiselet, L. Husson

Géosciences Rennes, Université de Rennes 1, CNRS, Campus de Beaulieu, Rennes, 35042 Cedex (France)

Summary

A striking feature of oceanic trench retreat is their convex arc shapes. Slab toroidal curvature is observed in nature, such as in the Sandwich subduction zone, and is described in several numerical and analogue models (Morra et al, 2006; Funiciello et al, 2003). However, we know little about the process responsible for this curvature, in part due to a lack of constraints but also to our poor understanding of the basic physics of the problem.
We note, however, that the toroidal curvature is not limited to the surface trench geometry. Many observations (mostly coming from tomographic images of the mantle) suggest that the toroidal curvature of the slab propagates to great depths into the mantle. Furthermore, this curvature seems to be conditionned by the width of the slab (Schellart et al, 2007). We suggest here that this process could be controlled by the rheology of the subducting plate.
Many studies have focused on the deformation of the slab in the poloidal plane (i.e., the subduction plane). Here, we explore the response of a subducting/retreating lithosphere in a longitudinal plane (i.e., perpendicular to the slab plane) and subjected to a toroidal mantle flow. To do so, we have developed a semi-analytical method based on the solution of the Stokes equation and the computation of a stream function, to better describe the toroidal mantle flow around the plate and, simultaneously, characterize the deformation of the slab. We solve the biharmonic stream function for incompressible Stokes flow in a square domain of width *5W*, where *W* is the width of the slab:

$$\nabla^4 \Psi = 0$$

with $u = -\partial\psi/\partial y$ and $v = \partial\psi/\partial x$, *u* and *v* being the velocities along the *x*- and *y*- cartesian coordinates. We impose that the vertical slab of width *W* retreats at a prescribed mean velocity V_t (see Figure 1). The local, along-strike velocity, is iteratively computed in order to be proportional to the deviatoric stress. This method allows to calculate the velocities in the mantle as well as the forces exerted by the mantle on the slab, and the dissipated energy in the mantle surrounding the slab. On Figure 2, we show the computed deviatoric stress during retreat of the slab. For an isoviscous case, the stress field evolves rapidly in the vicinity of the slab. As shown in Figure 2, compressional (positive) stress induced by the retreat of the slab is localized along the edge of the slab. Close to the corners of the slab, extensional stress (negative) are present. This phenomenon establishes a stress field compatible with the slab deformation. By integrating this solution through time, we are able to compute the evolution of the deformation on the slab (black line in Figure 2). In Figure 3a, we show the evolution of the deformation of the slab after 20 steps. Comparison of these results with seismic data (Figure 3b) allows to estimate, to first order, the rheology of the slab (i.e., viscosity contrast with the surrounding mantle). This model will lead to a better understanding of the interaction between the toroidal mantle flow and the slab behavior (deformation), as well as an estimate of the energy associated with the folding of the slab.